# Imaging the Absolute Configuration of a Chiral Epoxide in the Gas Phase

Philipp Herwig,[1]* Kerstin Zawatzky,[2]* Manfred Grieser,[1] Oded Heber,[3] Brandon Jordon-Thaden,[1] Claude Krantz,[1] Oldřich Novotný,[1,4] Roland Repnow,[1] Volker Schurig,[5] Dirk Schwalm,[1,3] Zeev Vager,[3] Andreas Wolf,[1] Oliver Trapp,[2]† Holger Kreckel[1]†

In chemistry and biology, chirality, or handedness, refers to molecules that exist in two spatial configurations that are incongruent mirror images of one another. Almost all biologically active molecules are chiral, and the correct determination of their absolute configuration is essential for the understanding and the development of processes involving chiral molecules. Anomalous x-ray diffraction and vibrational optical activity measurements are broadly used to determine absolute configurations of solid or liquid samples. Determining absolute configurations of chiral molecules in the gas phase is still a formidable challenge. Here we demonstrate the determination of the absolute configuration of isotopically labeled (*R*,*R*)-2,3-dideuterooxirane by foil-induced Coulomb explosion imaging of individual molecules. Our technique provides unambiguous and direct access to the absolute configuration of small gas-phase species, including ions and molecular fragments.

In 1847, Louis Pasteur realized that crystals of tartaric acid can come in two different shapes, which are nonsuperimposable mirror images of one another. He was able to sort them and dissolve them separately, and he found that the respective liquids rotate the axis of linearly polarized light in opposite directions. These simple experiments may be considered the birth of modern stereochemistry. A much greater challenge is to relate the sense of rotation of the polarization axis (the optical activity) to the handedness of the underlying microscopic molecular structure, which is referred to as the absolute configuration. Emil Fischer, who postulated the lock-and-key model of enzyme interactions in 1894 (*1*), realized that it was impossible to infer the absolute configuration from macroscopic models, and thus he arbitrarily defined dextrorotatory glucose as having *d*-configuration. It took more than 50 years until his guess was confirmed in 1951 when Bijvoet introduced anomalous single-crystal x-ray diffraction (XRD) to determine the absolute configuration of sodium rubidium tartrate (*2*). To this date, anomalous XRD is still the method of choice for absolute configuration measurements in crystalline samples.

More recently, vibrational circular dichroism (VCD) and vibrational Raman optical activity (ROA) have been used intensely to determine absolute configurations (*3*–*9*). Advances in computational chemistry allow simulating and predicting the spectral difference between the enantiomers by ab initio calculations. Lahav *et al*. introduced stereoselective habit modifications of crystals forming conglomerates to determine absolute configurations by surface interactions (*10*, *11*). Furthermore, microscopic techniques can be used to determine the sense of chirality of surface adsorbed molecules (*12*). All of the above methods have been used for important contributions, and an entire atlas of stereochemical information can be found in the literature (*13*). Nevertheless, difficulties remain for molecules that do not contain heavy atoms, and misassignments still occur, even in state-of-the-art laboratory studies (*14*). Moreover, to this date, the direct visualization of the absolute configuration of selected enantiomers in the gas phase has been elusive.

To address this stereochemical challenge, we developed the idea of using the foil-induced Coulomb explosion imaging (CEI) technique (*15*) to determine the handedness of a sample of individual chiral gas-phase molecules. In CEI experiments, the binding electrons of fast molecular ions are stripped off during passage through an ultrathin diamond-like carbon foil. The remaining positively charged atoms experience strong Coulomb repulsion, which leads to a magnification of the molecular structure that is recorded with modern imaging techniques (Fig. 1).

Very recently, Pitzer *et al*. (*16*) independently reported a similar approach using cold target recoil ion momentum spectroscopy (COLTRIMS) after laser-induced Coulomb explosion. In these studies, an effusive molecular beam is ionized by intense laser light. For this approach, sophisticated laser systems with sufficiently high intensities and repetition rates are necessary, owing to the rather inefficient ionization process. As the Coulomb explosion is triggered by 40-fs-long laser pulses, the time scale for the successive removal of the electrons is slow with respect to the vibrational movements of lighter species, like hydrogen and deuterium, within a given molecule. Therefore, those light nuclei cannot be considered static during the ionization process (*16*), which presently limits the technique to molecules made of heavier atoms. Moreover, large quantities of chiral gases are required, and thus only measurements with racemic mixtures of bromochlorofluoromethane and isotopically chiral bromodichloromethane were reported.

The foil-induced Coulomb explosion method described here, by contrast, requires only small sample amounts of chiral molecules (less than 100 mg was used for the present experiments). Given the well-known electron loss cross sections in fast atomic collisions (*17*), the ionization process due to electron stripping in the foil has a very high efficiency. Moreover, the ionization of all atomic fragments occurs simultaneously upon impact on the foil, within the first femtosecond (*15*). This is considerably faster than molecular vibration and rotation, and the position of all nuclei can be considered frozen during the stripping process. As we demonstrate here, this enables us to perform experiments with fundamental molecular species like epoxides, where the stereochemical information is carried by light atoms exclusively.

The CEI technique relies on time- and position-sensitive detection of all relevant fragments resulting from single-molecule breakup events [details of the experimental setup are given in (*18*, *19*)], and it has been used successfully to infer accurate information on the structure of diatomic molecules and simple polyatomics (*20*–*22*). To extend its range to species complex enough to exhibit chirality, we introduced ultrathin charge conversion

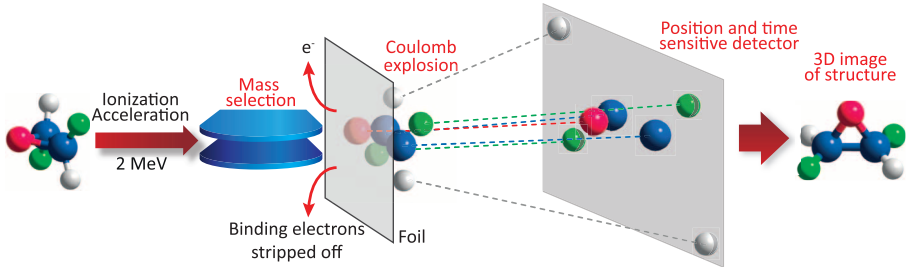


**Fig. 1. Determination of the absolute configuration of chiral molecules by foil-induced Coulomb explosion imaging.** Chiral molecules are ionized and accelerated, followed by mass selection to investigate only selected molecular ions or fragments. The Coulomb explosion is triggered by passing the molecules through an ultrathin stripping foil. The resulting charged atomic ions are recorded by a detector with high spatial and temporal resolution, revealing the molecular structure.

[1]Max-Planck-Institut für Kernphysik, 69117 Heidelberg, Germany. [2]Organisch-Chemisches Institut, Ruprecht-Karls Universität Heidelberg, 69120 Heidelberg, Germany. [3]Department of Particle Physics and Astrophysics, Weizmann Institute, 76100 Rehovot, Israel. [4]Columbia Astrophysics Laboratory, Columbia University, New York, NY 10027, USA. [5]Institut für Organische Chemie, Eberhard Karls Universität Tübingen, 72076 Tübingen, Germany.

*These authors contributed equally to this work.
†Corresponding author. E-mail: holger.kreckel@mpi-hd.mpg.de (H.K.); trapp@oci.uni-heidelberg.de (O.T.)

foils in front of both microchannel plate (MCP) detectors to increase the detection efficiency and developed improved parallel amplifiers to provide cross-talk–free multihit capabilities for each detector.

To meet the particular challenge of determining the absolute configuration of a molecule composed of lighter atoms, we chose *trans*-2,3-dideuterooxirane (compound **1**, Fig. 2A) as our target molecule. For this fundamental epoxide, the chiral character is introduced by two deuterons. The chosen compound **1** is a relatively rigid molecule and shows rotational symmetry ($C_2$), making the two stereogenic centers equivalent. Ionization of **1** by electron impact (fig. S5) does not affect the stereogenic centers, e.g., by bond dissociation. Moreover, unintended inversion of one of the stereogenic centers, e.g., by accidental exchange of the positions of H and D, results in the formation of achiral *cis*-2,3-dideuterooxirane, which would lead to an achiral contribution but not jeopardize the outcome of the experiment. Likewise, statistical double inversion would lead to a racemic sample accompanied by the formation of the achiral *cis*-2,3-dideuterooxirane isomer.

Samples of (*R*,*R*)-2,3-dideuterooxirane (***R*,*R*)-1** were prepared (*23*, *24*) according to an optimized eight-step synthetic protocol (fig. S4). The key step of the synthesis (Fig. 2B) is the enantioselective epoxidation of **2** by a modified semicatalytic Sharpless procedure (*25*) using titanium(IV) tetraisopropoxide, (+)-diisopropyl tartrate, and *tert*-butyl hydroperoxide. The configuration of the epoxide formed by the Sharpless asymmetric epoxidation is predictable, because the conversion is controlled by the configuration of the tartrate in the active complex. Therefore, under the reaction conditions described here, the (*S*,*S*)-configured epoxide **3** is formed with an enantiopurity of 97.5% (enantiomeric ratio). Mild oxidation of the alcohol by a Parikh-Doering reaction (*26*), employing a pyridine sulfur trioxide complex, gives the corresponding aldehyde in excellent yield. This step was followed by decarbonylation of the aldehyde group by stoichiometric reaction with the Wilkinson catalyst (*27*) $RhCl(PPh_3)_3$, under conservation of the stereogenic center at C2 of (***S*,*S*)-4**. Finally, (***R*,*R*)-1** is released as a gas by deprotection of the triphenylsilyl group using tetraethylammonium fluoride.

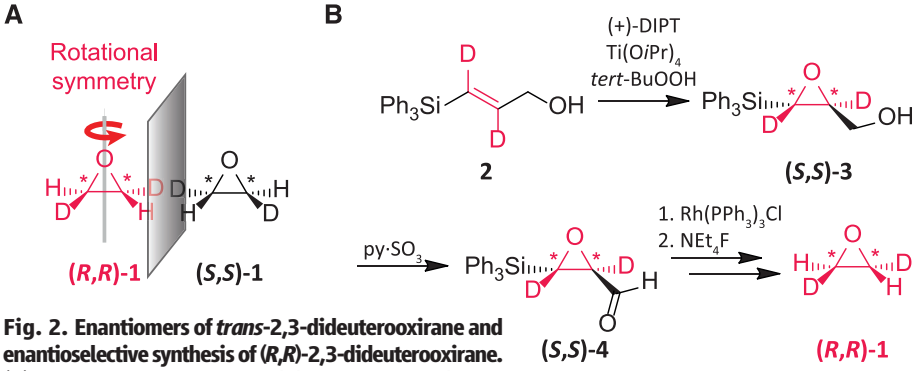


**Fig. 2. Enantiomers of *trans*-2,3-dideuterooxirane and enantioselective synthesis of (*R*,*R*)-2,3-dideuterooxirane.** (**A**) Enantiomers of *trans*-2,3-dideuterooxirane. The rotational symmetry is indicated by the rotation axis. (**B**) Asymmetric synthesis of the target molecule (*R*,*R*)-2,3-dideuterooxirane (***R*,*R*)-1** via a catalytic Sharpless epoxidation of deuterated allyl alcohol **2** as the key step of the synthetic sequence.

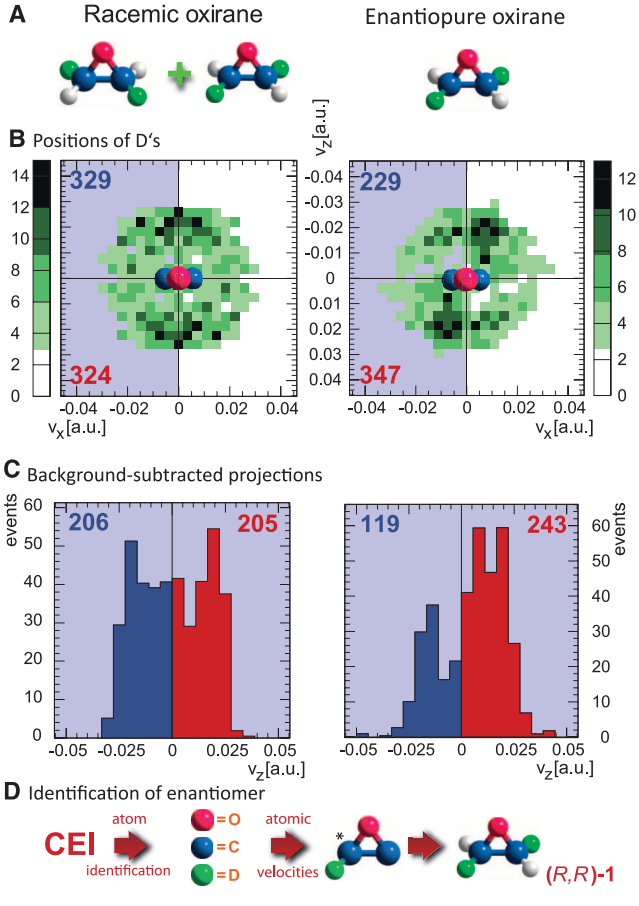


**Fig. 3. Imaging results and absolute configuration of *trans*-2,3-dideuterooxirane 1.** (**A**) CEI measurements were carried out for both enantiopure and racemic **1**. (**B**) Distribution of the D-atom velocities in the $v_x$-$v_z$ plane. This plane contains both C atoms and is oriented perpendicular to the C-O-C plane (the O atom, facing the viewer, is colored red). A distinct difference between racemic and enantiopure **1** is visible in the direction of the D-atom velocities. Accumulated event counts are given for relevant quadrants. (**C**) Projection of the blue areas onto the $v_z$ axis after subtraction of systematic background (see text and supplementary materials for definition). Whereas racemic **1** shows no propensity in the sign of $v_z$, the enantiopure sample reveals a clear precedence toward positive $v_z$ values. (**D**) The imaging results of enantiopure **1** unambiguously identify the configuration as (***R*,*R*)-1**.

The imaging results for both the racemic and the enantiopure oxirane (***R*,*R*)-1** samples are compared in Fig. 3. The coordinate system for each individual event is chosen such that the two C-atom

To obtain direct three-dimensional images of the *trans*-2,3-dideuterooxirane molecules, we ionized samples of racemic and enantiopure **1** in a standard cold cathode ion source. The resulting $C_2H_2D_2O^+$ ions were accelerated to 2.0 MeV, mass-selected, and then magnetically guided onto a thin (~5 nm) carbon foil (Fig. 1). Upon impact on the foil, the binding electrons are stripped off within less than a femtosecond, during which the position of the nuclei can be considered frozen. Behind the foil, the mutual Coulomb potential energy is rapidly converted to kinetic energy. For each individual molecular breakup, a dedicated detector system records the particle distances and impact times, which are proportional to the asymptotic velocities of the Coulomb explosion process. Because the purely repulsive dissociation conserves the handedness, the fragment velocities reflect the chirality of the molecules before fragmentation. As for the heavier atoms various charge states emerge from the foil, we used a magnetic separation field to select and separate the $C^{2+}$ and $O^{2+}$ charge states and to direct them onto a rectangular MCP detector at small deflection angles, whereas the $D^+$ ions were deflected more strongly onto a second, round detector (the $H^+$ ions were diverted outside of the detector region, fig. S1). By reversing the magnetic deflection in the data analysis, we reconstructed the three-membered C-O-C skeleton for events containing all three heavy fragments in the respective $X^{2+}$ charge state. Then the velocity of a single $D^+$ ion of the same event was determined with respect to this skeleton, defining the handedness of the corresponding stereogenic center. To rule out systematic uncertainties and detector effects, we performed control measurements with racemic *trans*-2,3-dideuterooxirane (fig. S3).

velocities lie on the $v_x$ axis, and the velocity of the C-O-C center of mass lies on the positive $v_y$ axis. The breakup velocity of the D atom is projected into the $v_x$-$v_z$ plane. The resulting distributions (Fig. 3B) reveal a clear difference in the absolute configuration of the two samples. Through the rotational symmetry of 2,3-dideuterooxirane (Fig. 2A), each event leads to two entries in the measured distribution, such that each half plane contains all information. To obtain a quantifiable parameter for the certainty with which we can determine the handedness of the enantiopure sample, we projected the blue area ($v_x < 0$) onto the $v_z$ axis (Fig. 3C). In this representation, a negative sign of $v_z$ corresponds to (*S*,*S*) symmetry, whereas a positive sign corresponds to (*R*,*R*) symmetry. Although events with both signs are seen (owing to molecular vibration and racemization induced in the ion source), this plot clearly identifies the enantiopure sample as (*R*,*R*)-2,3-dideuterooxirane (***R*,*R*)-1** with a statistical confidence level of 5σ. A systematic source of background, due to overlapping detector regions for $C^{2+}$ and $O^{2+}$, has been simulated and subtracted for Fig. 3C (see supplementary materials).

Our work uses direct imaging of a small gas-phase chiral compound to assign its sense of chirality. This offers a universal and self-consistent pathway to determine the absolute configuration of chemical species that may not be accessible by other methods. Imaging of chiral ionic species, as demonstrated here, can be combined with mass spectroscopic techniques to preselect molecules of a desired mass/charge ratio. Mass selectivity is an important feature of our approach, as it would enable us to measure gases containing large amounts of impurities, up to samples containing only small traces of chiral molecules. Furthermore, because we mass-select also the atomic fragments after Coulomb explosion and measure them in coincidence, this would permit us to discriminate against unwanted contamination by molecules with the same total mass but different atomic constituents. It would also be possible to store the ions between the initial ionization and the CEI measurement to accumulate and select a desired species or reaction product. Ion storage at cryogenic temperatures could be used to suppress internal excitations and thus provide more rigid molecular structures, which would make quantifiable measurements of the sample purity and the degree of racemization possible. Compared to macroscopic analysis techniques, only small quantities of the chiral species are needed, and neither optical activity nor crystalline samples are required. The foil-induced ionization process is universal and, as it does not rely on laser interactions or high sample densities, potentially can be applied to neutrals, ions, and radicals alike. With these properties, direct imaging of more complex chiral molecules can be envisioned in the future. Chemical compounds could be mass-selected at high resolution before their chiral properties are determined by applying ion-beam imaging. This paves the way for promising concepts of chiral sequencing and for highly efficient analysis of the absolute configuration of molecular fragments and reaction products.

By providing direct snapshots of selected enantiomers, our approach gives access to the absolute configuration of small gas-phase molecules, fully independent of quantum-chemical calculations. In addition, it offers broader intellectual merit in the direct visualization of a property as fundamental as chirality, on a molecular level.

### References and Notes


1. E. Fischer, *Ber. Dtsch. Chem. Ges* **27**, 2985–2993 (1894).
2. J. M. Bijvoet, A. F. Peerdeman, A. J. van Bommel, *Nature* **168**, 271–272 (1951).
3. P. J. Stephens, *J. Phys. Chem.* **89**, 748–752 (1985).
4. T. B. Freedman, X. Cao, R. K. Dukor, L. A. Nafie, *Chirality* **15**, 743–758 (2003).
5. P. J. Stephens, F. J. Devlin, J.-J. Pan, *Chirality* **20**, 643–663 (2008).
6. L. D. Barron, M. P. Bogaard, A. D. Buckingham, *J. Am. Chem. Soc.* **95**, 603–605 (1973).
7. J. Haesler, I. Schindelholz, E. Riguet, C. G. Bochet, W. Hug, *Nature* **446**, 526–529 (2007).
8. L. D. Barron, A. D. Buckingham, *Chem. Phys. Lett.* **492**, 199–213 (2010).
9. Y. He, B. Wang, R. K. Dukor, L. A. Nafie, *Appl. Spectrosc.* **65**, 699–723 (2011).
10. L. Addadi *et al.*, *Nature* **296**, 21–26 (1982).
11. Z. Berkovitch-Yellin, L. Addadi, M. Idelson, L. Leiserowitz, M. Lahav, *Nature* **296**, 27–34 (1982).
12. H. Fang, L. C. Giancarlo, G. W. Flynn, *J. Phys. Chem. B* **102**, 7311–7315 (1998).
13. W. Klyne, J. Buckingham, *Atlas of Stereochemistry—Absolute Configurations of Organic Molecules* (Chapman & Hall, London, 1978), vols. 1 and 2.
14. Y. Inokuma *et al.*, *Nature* **495**, 461–466 (2013).
15. Z. Vager, R. Naaman, E. P. Kanter, *Science* **244**, 426–431 (1989).
16. M. Pitzer *et al.*, *Science* **341**, 1096–1100 (2013).
17. V. S. Nikolaev, *Sov. Phys. Usp.* **8**, 269–294 (1965).
18. R. Wester *et al.*, *Nucl. Instrum. Methods Phys. Res. A* **413**, 379–396 (1998).
19. R. Wester *et al.*, *J. Chem. Phys.* **116**, 7000 (2002).
20. B. Jordon-Thaden *et al.*, *Phys. Rev. Lett.* **107**, 193003 (2011).
21. P. Herwig *et al.*, *Phys. Rev. A* **87**, 062513 (2013).
22. L. Lammich *et al.*, *Phys. Rev. A* **69**, 062904 (2004).
23. J. M. Schwab, C.-K. Ho, *J. Chem. Soc. Chem. Commun.* (11): 872 (1986).
24. J. M. Schwab, T. Ray, C.-K. Ho, *J. Am. Chem. Soc.* **111**, 1057–1063 (1989).
25. Y. Gao *et al.*, *J. Am. Chem. Soc.* **109**, 5765–5780 (1987).
26. J. R. Parikh, W. von E. Doering, *J. Am. Chem. Soc.* **89**, 5505–5507 (1967).
27. D. Evans, J. A. Osborn, F. H. Jardine, G. Wilkinson, *Nature* **208**, 1203–1204 (1965).


**Acknowledgments:** This work was supported by the Max-Planck Society and the Ruprecht-Karls Universität Heidelberg. O.N. was supported, in part, by grants from NASA and the NSF. H.K. and O.T. were supported by the European Research Council under Grant Agreements StG 307163 and StG 258740, respectively. D.S. acknowledges support by the Weizmann Institute through the Joseph Meyerhoff program. We thank B. F. Straub for support in the quantum-chemical calculations and F. Rominger for x-ray structure analysis. We thank G. Helmchen and H. Wadepohl for helpful discussions. We are grateful for the support from the Max-Planck-Institut für Kernphysik accelerator staff, and we thank O. Koschorreck for assistance with the CEI detector electronics. Metrical parameters for the crystal structures of compounds [**triphenylsilyl propargyl alcohol, 2,** (***S*,*S*)-3** and (***S*,*S*)-4**] are available free of charge from the Cambridge Crystallographic Data Centre under reference numbers CCDC 964292, CCDC 964293, CCDC 964294, and CCDC 964295, respectively.

### Supplementary Materials

www.sciencemag.org/content/342/6162/1084/suppl/DC1
Materials and Methods
Figs. S1 to S5
Appendix
References (*28*–*36*)

27 September 2013; accepted 29 October 2013
10.1126/science.1246549

# Regular Patterns in Frictional Resistance of Ice-Stream Beds Seen by Surface Data Inversion

**Olga V. Sergienko[1]* and Richard C. A. Hindmarsh[2]**

**Fast-flowing glaciers and ice streams are pathways for ice discharge from the interior of the Antarctic Ice Sheet to ice shelves, at rates controlled by conditions at the ice-bed interface. Using recently compiled high-resolution data sets and a standard inverse method, we computed basal shear stress distributions beneath Pine Island and Thwaites Glaciers, which are currently losing mass at an accelerating rate. The inversions reveal the presence of riblike patterns of very high basal shear stress embedded within much larger areas with zero basal shear stress. Their colocation with highs in the gradient of hydraulic potential suggests that subglacial water may control the evolution of these high–shear-stress ribs, potentially causing migration of the grounding line by changes in basal resistance in its vicinity.**

Observations from satellite and aircraft-based platforms show that the ice streams in Amundsen Sea Embayment are the greatest contributors to Antarctic ice-sheet mass loss (*1*, *2*), including Pine Island Glacier (PIG) and Thwaites Glacier (Fig. 1). In contrast to PIG, which flows in a trough whose lateral walls provide resistance to ice flow in addition to its bed, Thwaites is unconfined, with most resistance to its gravity-driven flow coming from its bed. The flux of ice through the grounding line, which determines the rate at which glaciers contribute to

[1]Program in Atmospheric and Oceanic Sciences, Princeton University, 201 Forrestal Road. Princeton, NJ 08540, USA. [2]British Antarctic Survey, High Cross, Madingley Road, Cambridge CB3 0ET, UK.

*Corresponding author. E-mail: osergien@princeton.edu

Editor's Summary

**Foil-Forged Images**

X-ray diffraction is widely used to determine molecular geometries and can often distinguish mirror image isomers (enantiomers), which generally requires well-ordered crystals. **Herwig *et al.*** (p. 1084) report an imaging technique to characterize enantiomers in the gas phase. A succession of ionization events were induced by passage through a carbon foil that culminated in a Coulomb explosion of mutually repelling nuclei. The trajectories of these nuclei precisely reflected the original molecular structure.